Light absorption distribution of prostate tissue irradiated by diffusing light source*

PENG Dong-qing (彭东青)[1,2], XIE Wen-ming (谢文明)[3], GUO Jian (郭建)[1], TANG Jia-ming (唐嘉铭)[1], LI Zhi-fang (李志芳)[1], and LI Hui (李晖)**

1. Key Laboratory of Optoelectronic Science and Technology for Medicine, Ministry of Education of China, Fujian Provincial Key Laboratory of Photonic Technology, College of Photonic and Electronic Engineering, Fujian Normal University, Fuzhou 350007, China

2. School of Science, Jimei University, Xiamen 361021, China

3. School of Information Science and Engineering, Fujian University of Technology, Fuzhou 350118, China

(Received 28 January 2015)

Determination of light absorption distribution in the prostate tissue irradiated by diffusing light source is important for the treatment planning. In this paper, a three-dimensional (3D) optical model of human prostate is developed, and the light absorption distribution in the prostate tissue is estimated by Monte Carlo simulation method. Light distribution patterns including 3D distributions in the tissue model irradiated by two diffusing light sources are obtained and compared. Also, the impacts of length and energy of cylinder diffusing light source on the irradiance volume are demonstrated. Those results will be significant for the nondestructive qualitative assessments of photodosimetry in biomedical phototherapy.

Document code: A **Article ID:** 1673-1905(2015)03-0237-4

DOI 10.1007/s11801-015-5020-3

In recent years, prostate cancer has been a serious health concern[1-3]. More and more attentions have been paid to the optical treatment of prostate cancer, including laser-induced interstitial thermotherapy (LITT)[4], photodynamic therapy (PDT)[5,6], etc. Using the interstitial light delivery technique, PDT has been used to treat large bulky tumors in solid organs bulky tumors or organs. Since the tumors of prostate are often confined to the prostate itself, several preclinical studies have evaluated the feasibility of delivering PDT to the prostate via the interstitial approach[7,8]. As an efficient illumination scheme for cylinder-like hollow organs, such as prostate, the interstitial light delivery is commonly employed in their treatment method of PDT. Owing to its advantage in illuminating a larger volume of target tissue than conventional fibers by attaching diffusing ends, the diffusing light source is widely applied in interstitial photodynamic therapy (iPDT). As we know, the absorption of light in an irradiated volume is the first stage of laser-tissue interaction, which determines the results of a medical treatment. Therefore, the determination of light absorption distribution in biological tissue contributes to selecting strategy and optimizing dose for biomedical application, such as PDT of tumors. As to iPDT, the accurate determination of the light absorption distribution from diffusing light source is important for the prediction of the outcome and the treatment planning, even the adjustments of laser parameters during irradiation.

There are already some methods to investigate the light distribution from a diffuser in biotissue, but no method has been used for invasive measurement in prostate tissue. T. C. Zhu et al[9,10] used an optical fiber-based isotropic detector to measure light fluence rate distribution in prostate, but its invasive procedure cannot meet practical applications. A video technique was introduced to reconstruct the light emission profile of diffuser in phantom by Ripley et al[11], but this method becomes very challenging and unreliable when the cylindrical diffuser is applied in deep tissues, such as the prostate. A photoacoustic method for the non-invasive estimation and reconstruction of three-dimensional (3D) light distribution produced by the cylindrical diffuser in biological was proposed by W. Xie et al[12]. But this method is still inconvenient and hard to be suitable for prostate tissue. Thus, the numerical modeling is still an important and effective way of gaining a deeper understanding of the complex interactions of the laser-tissue interaction process[13,14], and the numerical method is still widely used to simulate light transport in tissues for various applications[15-17]. T. M. Baran et al[17] presented a new Monte Carlo model of cylindrical diffusing fibers to simulate the irradiance around the diffuser based on physical construction of these fibers. However, so far, a complex prostate tissue optical model is not available.

In order to optimize the laser conditions of iPDT, the knowledge of absorbed light distribution in prostate tis-

* This work has been supported by the National Natural Science Foundation of China (Nos.61178089 and 81201124), the Fujian Provincial Key Program of Science and Technology (No.2011Y0019), the Fujian Provincial Education Science Research Project of Young Teachers (No.JA14189), and the Huang Huizhen Foundation for Discipline Construction in Jimei University (No.ZB2013068).

** E-mail: hli@fjnu.edu.cn

sue by diffusing light source is essential. In this paper, a 3D complex optical model of human prostate is combined with the Monte Carlo simulation method to provide the light absorption distribution by the diffuser radiation in the prostate tissue. And the propagation characteristics and light absorption distribution patterns in the tissue model respectively irradiated by a cylinder diffuser light source and a sphere diffuser light source are obtained and compared with each other. Also, the impacts of length and energy of cylinder diffuser light source on the irradiance volume are demonstrated.

Fig.1 is the illustration of the prostate structure and 3D mesh optical model of prostate by two diffusing light sources. As shown in Fig.1(a), the prostate looks like a chestnut, and the urethra is through the middle of the prostate. The 3D triangular mesh optical model of prostate is established through programming by Matlab software according to human prostate's morphology, as shown in Fig.1(b) and (c). The triangular meshes are expressed as off file. Off file uses the surface of object to represent the geometry of the object, and then the surface of the object is divided into a large number of triangles. The prostate phantom's transverse diameters at x-axis and y-axis and the height are about 2 cm, 4 cm and 3 cm, respectively, and its center is located at (0 mm, 0 mm, 15 mm). In order to meet the actual surrounding situation, a cube tissue is used to surround the prostate model. A Cartesian coordinate system is used for the simulation. And the main optical properties at wavelength of 732 nm for prostate optical model[5,9] are specified as the absorption coefficient of μ_{ap}=0.13 mm^{-1}, the reduced scattering coefficient of $\mu'_{sp}=\mu_{sp}(1-g_P)=0.19$ mm^{-1} and the tissue refractive index of n_p=1.43. The optical parameters of surrounding cube tissue are listed as μ_{as}=0.11 mm^{-1}, μ'_{ss}=1.0 mm^{-1} and n_s=1.43 at wavelength of 732 nm.

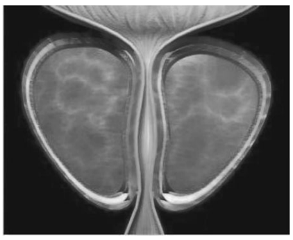

(a) Structure of prostate

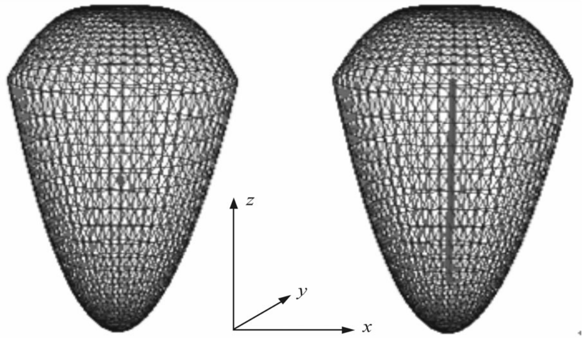

(b) Sphere diffusing light (c) Cylinder diffusing light

Fig.1 Prostate structure and 3D mesh prostate optical model by two diffusing light sources

The simulation process is shown in Refs.[18−20]. The record range of light absorption distribution in the Monte Carlo simulation is always kept as (−15 mm, 15 mm) at x-axis, (−25 mm, 25 mm) at y-axis and (−10 mm, 40 mm) at z-axis, and the record steps in three axes are set to be 0.3 mm, 0.5 mm and 0.5 mm, respectively.

For modeling interstitial light delivery through the urethra, a sphere diffusing light source with diameter of 0.6 mm and a cylinder diffusing light source with height of 2 cm and radius of 0.3 mm are set in the middle of the model, respectively, as shown in Fig.1(b) and (c). The wavelengths of the two continuous wave (CW) lasers are both set to be 732 nm. The total energy of incident light is set as 1 J, and the total number of incident photon packets is 500 000.

Light absorption distribution simulation results of two irradiation light sources in xz-plane and yz-plane are shown in Figs.2 and 3, respectively. Comparing Fig.2(a) with (b), it can be shown that the lateral scope of uniform absorbed light energy distribution within the prostate model irradiated by sphere diffusing light is much smaller than that irradiated by cylinder diffusing light. But its value of absorbed light energy near the center is larger. And the differences between Fig.3(a) and (b) are similar to those between Fig.2(a) and (b). But the light distribution range in yz-plane is much smaller than that in xz-plane. And it can be explained as the influence of boundary reflected by the photons. Since the length of prostate model at x-axis is smaller than the length at y-axis, more photons are reflected at the model boundary of which the refractive indices are mismatched. And these will lead to an increased backscattering probability, and thus there is a rise of light absorption near the boundary and a larger range of uniform light absorbed distribution.

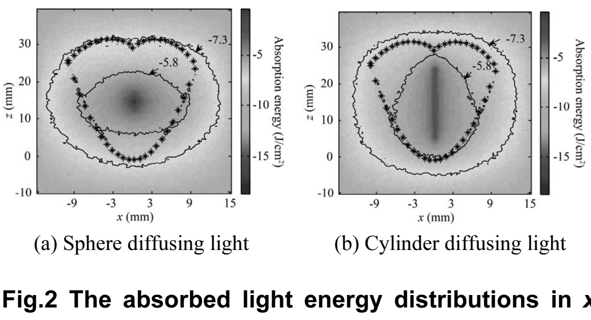

(a) Sphere diffusing light (b) Cylinder diffusing light

Fig.2 The absorbed light energy distributions in *xz*-plane produced by two light sources (The ∗ line is the boundary for prostate model, and two contour lines of light absorption energy present –5.8 J/cm^2 and –7.3 J/cm^2, respectively.)

A 3D distribution in the prostate tissue can be easily obtained. In Fig.4(a) and (b), the 3D distributions with four slices in the prostate tissue for sphere diffusing light and cylinder diffusing light are given, respectively. Since the irregular structure of prostate tissue, the boundary area becomes smaller when x-position of slice is large. The 3D light absorption distributions make all light absorption spatial distribution information in the prostate available.

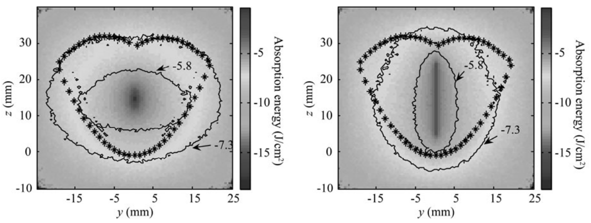

(a) Sphere diffusing light (b) Cylinder diffusing light

Fig.3 The absorbed light energy distributions in *yz*-plane produced by two light sources (The ∗ line is the boundary for prostate model, and two contour lines of light absorption energy present –5.8 J/cm^2 and –7.3 J/cm^2, respectively.)

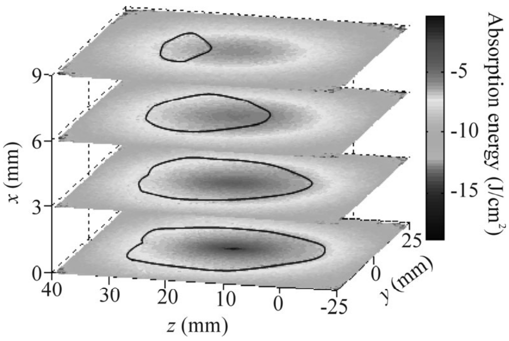

(a) Sphere diffusing light

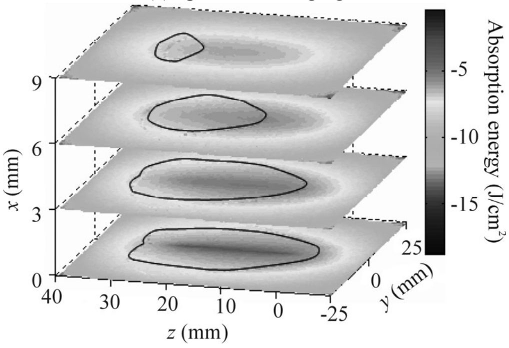

(b) Cylinder diffusing light

Fig.4 3D light absorption distribution in prostate tissue irradiated by two diffusing light sources (The black line is the boundary line for prostate model.)

In order to give a quantitative comparison of irradiance range of two kinds of diffusing light sources, two contour lines of the relative light absorption energy for –5.8 J/cm^2 and –7.3 J/cm^2 are drawn in Figs.2 and 3. The irradiance areas at absorption energy of –5.8 J/cm^2 for sphere diffusing light and cylinder diffusing light are 2.175 cm^2 and 2.755 cm^2 in *xz*-plane and 1.837 cm^2 and 2.478 cm^2 in *yz*-plane, respectively. As to the absorption energy of –7.3 J/cm^2, the irradiance areas for two light sources are 7.335 cm^2 and 8.274 cm^2 in *xz*-plane and 8. 562 cm^2 and 9.568 cm^2 in *yz*-plane, respectively. Thus, the irradiance volume can be calculated by summing up all sections. The irradiance volumes of sphere diffusing light and cylinder diffusing light are 2.093 cm^3 and 2.158 cm^3 at absorption energy of –5.8 J/cm^2, respectively, and those at absorption energy of –7.3 J/cm^2 are 15.703 cm^3 and 17.119 cm^3, respectively. These results show that the irradiance range of cylinder diffusing light source is larger than that of sphere diffusing light source, when their energy is the same.

The results of the irradiance volumes of those two light sources with different laser absorption energy of –5.8 J/cm^2 and –7.3 J/cm^2 are shown in Fig.5. It can be seen that there is a rough linear increase in irradiance volume as the increase of laser energy. And irradiance volume of cylinder diffusing light source is larger than that of sphere diffusing light source. As we know, as the laser energy increases, the initial light intensity increases proportionally, while the optical parameters of tissue model remain constant. As a result, the depth z at which the relative absorption energy can reach –5.8 J/cm^2 and –7.3 J/cm^2 will increase. Thus, the irradiance volumes of two diffusing light sources increase. Due to the sharp attenuation of light by diffusing light source, multi-fiber might be used to improve the incident laser energy in order to obtain an adequate irradiance volume.

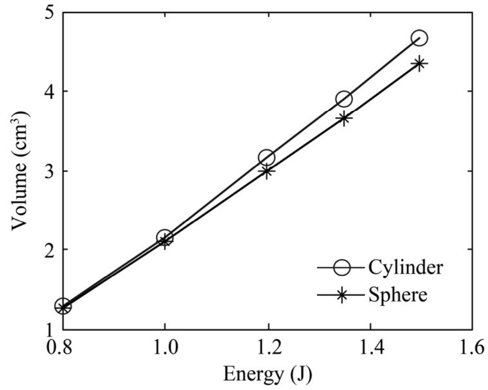

(a) –5.8 J/cm^2

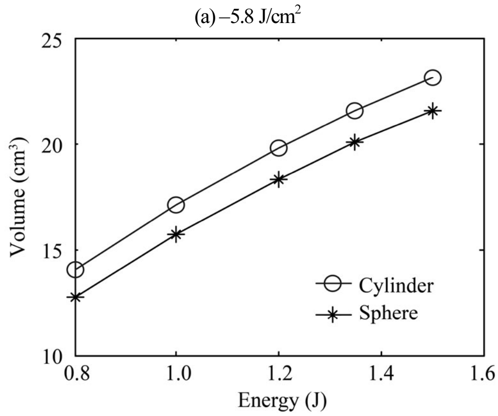

(b) –7.3 J/cm^2

Fig.5 Results of the irradiance volume with respect to laser energy for two relative absorption energy values

Likewise, the influence of length of cylinder diffusing light source on the irradiance volume is shown in Fig.6 for the relative absorption energy of –5.8 J/cm^2 and –7.3 J/cm^2.

Here, the laser energy is kept to be 1 J. Note that there is a linear slow increase in irradiance volume as the length increases in both Fig.6(a) and (b). This indicates that an optimal length of diffusing light should be adopted when the iPDT for prostate tissue is carried out.

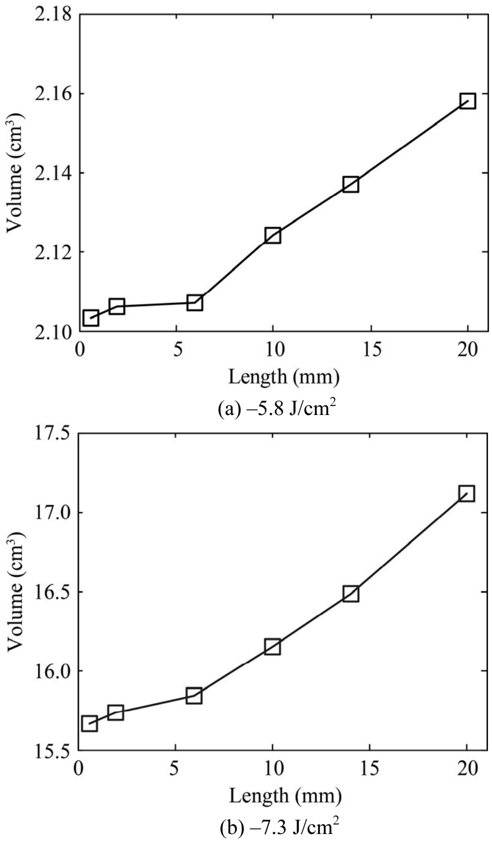

Fig.6 Results of the irradiance volume with respect to length of cylinder diffusing light for two absorption energy values

In this paper, an optical model of human prostate is employed, which is combined with Monte Carlo simulation method, to provide the light absorption distribution in the prostate tissue irradiated by diffusing light source. The impacts of length and energy of cylinder diffusing light source on the irradiance volume are demonstrated. The results show that there is a better uniform light distribution characteristic along the length of the cylinder diffusing light source. And the irradiance range of cylinder diffusing light is larger than that of sphere diffusing light. Moreover, laser energy and length both contribute to the irradiance range. The knowledge of light absorption distribution in prostate tissues might offer a reference dosage for PDT. This numerical method for a 3D optical model of a bio-tissue with complex structure combined with Monte Carlo simulation will also be useful to the quantitative prediction of the light absorption distribution in the biomedicine. Next step, the light distribution experimental system will be established, and the measurement of light absorption distribution in prostate tissue will be carried out from the prostate tissue phantom to in vitro prostate tissue.

References

[1] R. Siegel, D. Naishadham and A. Jemal, CA: A Cancer Journal for Clinicians **63**, 11 (2013).

[2] V. S. Dogra, B. K. Chinni, K. S. Valluru, J. V. Joseph, A. Ghazi, J. L. Yao, K. Evans, E. M. Messing and N. A. Rao, Journal of Clinical Imaging Science **3**, 41 (2013).

[3] N. Kuo, H. J. Kang, D. Y. Song, J. U. Kang and E. M. Boctor, Journal of Biomedical Optics **17**, 066005 (2012).

[4] S. C. Jiang and X. X. Zhang, Lasers in Medical Science **19**, 197 (2005).

[5] T. C. Zhu, S. M. Hahn, A. S. Kapatkin, A. Dimofte, C. E. Rodriguez, T. G. Vulcan, E. Glatstein and R. A. Hsi, Photochemistry and Photobiology **77**, 81 (2003).

[6] J. Li, M. D. Altschuler, S. M. Hahn and T. C. Zhu, Physics in Medicine and Biology **53**, 4107 (2008).

[7] L. K. Lee, C. Whitehurst, Q. Chen, M. L. Pantelides, F. W. Hetzel and J. V. Moore, British Journal of Urology **80**, 898 (1997).

[8] S. C. Chang, G. Buonaccorsi, A. MacRobert and S. G. Bown, International Journal of Cancer **67**, 555 (1996).

[9] T. C. Zhu, A. Dimofte, J. C. Finlay, D. Stripp, T. Busch, J. Miles, R. Whittington, S. B. Malkowicz, Z. Tochner, E. Glatstein and S. M. Hahn, Photochemistry and Photobiology **81**, 96 (2005).

[10] A. Dimofte, J. C. Finlay, X. Liang and T. Zhu, Physics in Medicine and Biology **57**, 6025 (2012).

[11] P. M. Ripley, T. N. Mills and J. A. S. Brookes, Lasers in Medical Science **14**, 67(1999).

[12] W. Xie, Y. Liu, Z. Li and H. Li, Chinese Optics Letters **12**, 051702 (2012).

[13] YANG Bo-zan, YANG Chun-mei, SA Yu, DING Jun-hua, LI Mei-hua, LIANG Xiao-hui, FENG Yuan-ming and HU Xin-hua, Journal of Optoelectronics·Laser **25**, 2437 (2014). (in Chinese)

[14] XU De-gang, LIU Chang-ming, WANG Yu-ye, WANG Wei-peng, JIANG Hao, ZHANG Zhuo, LIU Peng-xiang and YAO Jian-quan, Optoelectronics Letters **9**, 73 (2013).

[15] A. Shirkavand, S. Sarkar, M. Hejazi, L. A. Fashtami and M. R. linaghizadeh, Chinese Optics Letters **5**, 238 (2007).

[16] Y. Chen, X. Ma, X. Wang and S. Wang, Chinese Optics Letters **12**, S22201 (2014).

[17] T. M. Baran and T. H. Foster, Journal of Biomedical Optics **16**, 085003 (2011).

[18] L. Wang, S. L. Jacques and L. Zheng, Computer Methods and Programs in Biomedicine **47**, 131 (1995).

[19] H. Li, J. Tian, F. Zhu, W. Cong, L. V. Wang, E. A. Hoffman and G. Wang, Academic Radiology **11**, 1029 (2004).

[20] X. Chen, X. Gao, X. Qu, J. Liang, L. Wang, D. Yang, A. Garofalakis, J. Ripoll and J. Tian, Optics Express **17**, 16266 (2009).